Kinetic Modeling of Benzene Decomposition Near 1000 K: The Effects of Toluene Impurity

M. G. BRIOUKOV, J. PARK, M. C. LIN

Department of Chemistry, Emory University, Atlanta, Georgia 30322

Received 29 September 1997; accepted 31 March 1999

ABSTRACT: Kinetic data of Brooks et al. [3] on the decomposition of C_6H_6 near 1000 K have been analyzed by computer modeling. The observed overall 3/2-order kinetics could be accounted for by a mechanism composed of 4 key reactions involving H atoms and C_6H_5 radicals using recently acquired rate constants. However, the appearance of CH_4 and the enhanced H_2 yields could only be explained by invoking the reactions of ~0.1% of toluene present in the system as reported by the authors. Overall, the decomposition reaction is dominated by the unimolecular dissociation of C_6H_6 followed by the short chain process, $H + C_6H_6 = C_6H_5 + H_2$ and $C_6H_5 + C_6H_6 = C_{12}H_{10} + H$, which result in the dehydrogenation of C_6H_6, producing $C_{12}H_{10} + H_2$. In order to account for the yield of H_2 quantitatively, the displacement reaction, $C_6H_5CH_2 + C_6H_6 = CH_2(C_6H_5)_2 + H$, was invoked and modeled to have the approximate rate constant, $8.4 \times 10^{11} \exp(-11800/T)$ cm^3 mol^{-1} s^{-1}. © 1999 John Wiley & Sons, Inc. Int J Chem Kinet 31: 577–582, 1999

INTRODUCTION

The kinetics and mechanism of benzene decomposition reaction is relevant to the combustion chemistry of hydrocarbons in conjunction with the formation of soot in its incipient stages [1,2]. The thermal decomposition reaction has been investigated by many laboratories using a variety of techniques [3–8]. At temperatures above 1200 K, the reaction becomes complex and is dominated by ring-opening processes. At temperatures between 900 and 1200 K, the dehydrogenation reactions producing $H_2 + C_{12}H_{10}$ (biphenyl) are dominant [3].

This study is focused on the elucidation of the mechanism for the dehydrogenation process occurring in the vicinity of 1000 K, which is controlled primarily by the initiation reaction. In this lower temperature regime ($T \leq 1200$ K), the ring-opening processes are relatively unimportant and the overall mechanism involves only a handful of reaction steps, which have been recently studied experimentally and theoretically with sufficient reliability. For example, for the first few steps of the decomposition mechanism [3]:

$$C_6H_6 \longrightarrow C_6H_5 + H \tag{1}$$

$$C_6H_6 + H \longrightarrow C_6H_5 + H_2 \tag{2}$$

$$C_6H_5 + C_6H_6 \longrightarrow C_{12}H_{10} + H \tag{3}$$

$$C_6H_5 + C_6H_5 \longrightarrow C_{12}H_{10} \tag{4}$$

their rate constants have been determined (see later) and are employed in this study for kinetic modeling

---

Correspondence to: M. G. Brioukov (chemmcl@emory.edu)

Contract grant sponsor: Basic Energy Sciences, Department of Energy
Contract grant number: DE-FG02-97-ER14784

of H_2 production measured by Brooks and coworkers [3].

The results of this study indicate that the overall rate constants for the production of hydrogen, which obeys the 3/2-order rate law,

$$d[H_2]/dt = k\,[C_6H_6]^{3/2}$$

with $k = 10^{9.93} \exp(-53{,}790/T)$ dm^3 mol$^{-1/2}$ s^{-1}, is strongly influenced by the ~0.1% of toluene impurity present in their reaction mixtures. The effect was examined by computer simulation and the results presented herein.

KINETIC MODELING

The kinetic data obtained from the pyrolysis of benzene in a static reactor in the temperature range of 910–1157 K by Brooks and coworkers [3] were modeled with recently established rate constants for the key elementary steps, including reaction (1)–(4) employed in their original analysis.

Steady-state assumption for [H] and $[C_6H_5]$ employing (1)–(4) led to the observed 3/2-order kinetic (see Fig. 1) for H_2 production [3]:

$$d[H_2]/dt = k_1\,[C_6H_6] + k_2\,(k_1/k_4)^{1/2}\,[C_6H_6]^{3/2} \qquad \text{(I)}$$

provided that the initiation rate, $k_1[C_6H_6]$, is small in comparison with the chain-propagation rate. The assumption is valid on account of the high C–H bond strength in benzene and zero intercept revealed by Figure 1. Accordingly equation (I) can in principle be utilized to analyze the observed kinetic data and to evaluate k_1 or k_2, for example.

At that time, the authors were unable to accomplish this analysis because of the absence of reliable values for all three rate constants. They have since been determined directly by experiments or indirectly through kinetic modeling or theoretical calculations. Reaction (1) or its reverse process has been determined by several groups [7–11]. Recently, reaction (2) was calculated by us with ab initio molecular orbital and statistical theory [12]. The computed reverse rate constant (k_{-2}) has been shown to agree with experimentally measured data [13]. Reaction (3), first studied by Fahr and Stein [14], has been measured in its reverse direction by Manion and Tsang [15]. These data are kinetically consistent. Recently, three independent sets of data have been reported for reaction (4) [16–18]. The result of Park and Lin [16], which covers a broader 1/*T* range, lies in the middle with the values which can be represented by $k_4 = 1.38 \times 10^{13}\,e^{-55/T}$ cm^3 mol^{-1} s^{-1}.

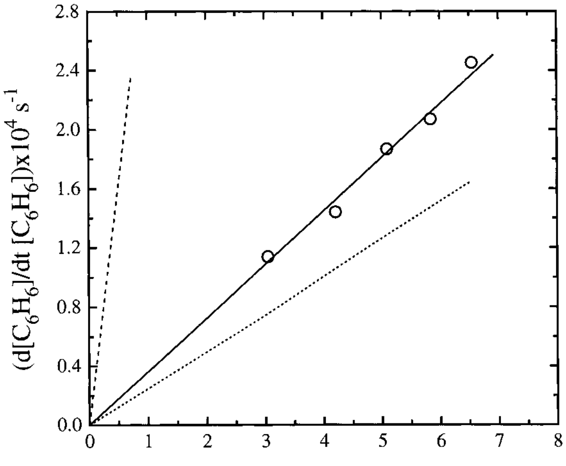

Figure 1 Function plot to test proposed mechanism at 993 K. Dashed line, kinetically modeled H_2 yield excluding the reversible reaction of reaction (1); dotted line, kinetically modeled H_2 yield including the reversible reaction of reaction (1). The experimental data was reproduced from Figure 8 of Ref. 3.

The employment of the "best" kinetic data (shown in Table I) including our recent measurements on reaction (7) and (13) [19,20] to account for the H_2 production presented in Fig. 1 with equation (I), however, leads to a significantly higher yield than the observed one as indicated by the dashed line. The large deviation results essentially from the exclusion of reverse reactions, particularly (−1). The inclusion of all reverse processes in the scheme as required by modeling with the CHEMKIN/SENKIN program [21,22] reduces the H_2 production below the experimental values as illustrated by the dotted line. For kinetic modeling the thermodynamic property of C_6H_5 was obtained by using the recent ab initio result by Mebel et al. [12] and those of $CH_2(C_6H_5)_2$ and $CH(C_6H_5)_2$ were obtained by using Melius' BAC-MP2 results [23]. All other thermodynamic properties were taken directly from CHEMKIN/SENKIN thermodynamic library. Figure 2 further demonstrates the underestimation of kinetically modeled results in H_2 production by dashed (967 K) and dotted (910 K) lines. The deviation between the experiment and the modeled result using the four reversible reactions may be attributed to the presence of the ~0.1% of $C_6H_5CH_3$ impurity in the mixture as reported by the original authors [3].

Aside from the major toluene reactions responsible for the enhanced initiation rate [reaction (−5) and

Table I The Reactions and Rate Constants Used in the Modeling of Considered Kinetic Data[a]

Reactions	A	n	E	Ref.
1. $C_6H_5 + H = C_6H_6$	7.83×10^{13}	0.0	0	26
2. $C_6H_5 + H_2 = C_6H_6 + H$	5.71×10^{4}	2.43	6280	12
3. $C_{12}H_{10} + H = C_6H_5 + C_6H_6$	4.10×10^{13}	0.0	8780	15
4. $2C_6H_5 = C_{12}H_{10}$	1.39×10^{13}	0.0	111	16
5. $C_6H_6CH_2 + H = C_6H_5CH_3$	1.50×10^{14}	0.0	0	27
6. $C_6H_5 + CH_3 = C_6H_5CH_3$	1.39×10^{13}	0.0	30	20
7. $C_6H_5 + C_6H_5CH_3 = C_6H_6 + C_6H_5CH_2$	2.70×10^{-1}	4.02	-1590	19
8. $C_6H_5CH_2 + C_6H_6 = CH_2(C_6H_5)_2 + H$	8.35×10^{11}	0.0	23506	This work
9. $CH_2(C_6H_5)_2 \rightarrow C_{13}H_{10} + H_2$	1.00×10^{8}	0.0	35000	24
10. $C_6H_5CH_3 + H = C_6H_5CH_2 + H_2$	3.97×10^{2}	3.4	3120	26
11. $C_6H_5CH_3 + H = C_6H_6 + CH_3$	6.62×10^{2}	3.0	749	26
12. $CH_3 + C_6H_5CH_3 = C_6H_6CH_2 + CH_4$	1.17×10^{11}	0.0	8000	28
13. $C_6H_5 + CH_4 = CH_3 + C_6H_6$	3.90×10^{-3}	4.57	10460	20
14. $H + CH_4 = CH_3 + H_2$	1.32×10^{4}	3.0	8040	26
15. $C_6H_5CH_2 + C_6H_5 = CH_2(C_6H_5)_2$	1.00×10^{13}	0.0	0	b
16. $CH(C_6H_5)_2 + H = CH_2(C_6H_5)_2$	1.00×10^{14}	0.0	0	b
17. $2C_7H_7 = H = C_{14}H_{14}$	2.51×10^{11}	0.4	0	29
18. $C_6H_5CH_2 + CH_3 = C_6H_5CH_2CH_3$	1.19×10^{13}	0.0	220	30
19. $2H + M = H_2 + M$	5.40×10^{18}	-1.3	0	31
20. $2CH_3(+M) = C_2H_6(+M)$ LOW / 1.770E + 50 −9.670 6220.00/ TROE /.5325 151.00 1038.00 4970.00/ CH_4/2.00/C_6H_6/3.00/	3.61×10^{13}	0.0	0	26
21. $CH_3 + H(+M) = CH_4(+M)$ LOW / 2.477E + 33 −4.760 2440.00/ TROE / .7830 74.00 2941.00 6964.00/ CH_4/2.00/C_6H_6/3.00/	1.27×10^{16}	-0.63	383	26

[a] The tabulated rate constants are defined by $k(T) = AT^n \exp(-E_a/RT)$, where E_a is in cal/mol and $k(T)$ is in $cm^6\ mol^{-1}\ s^{-1}$ for third-order reactions, $cm^3\ mol^{-1}\ s^{-1}$ for second-order reactions and in s^{-1} for first-order reactions. The equal sign in each reaction indicates that both forward and reverse reactions are included in the modeling.

[b] Reaction rate constants are kinetic estimations based on our literature review for combination reactions.

(-6)] as well as the production of CH_3 [reaction (-6) and (11)], $C_6H_5CH_3$ may also inhibit the formation of H_2 by the following reactions:

$$C_6H_5CH_2 + H = C_6H_5CH_3 \tag{5}$$

$$C_6H_5 + CH_3 = C_6H_5CH_3 \tag{6}$$

$$C_6H_5 + C_6H_5CH_3 = C_6H_6 + C_6H_5CH_2 \tag{7}$$

However, the inclusion of these reactions still led to a slight underestimation of the H_2 yield assuming that the 0.1% of toluene impurity remained constant in the mixture. In order to account for high concentration of H_2 yield we introduced the following two likely reactions:

$$C_6H_5CH_2 + C_6H_6 = CH_2(C_6H_5)_2 + H \tag{8}$$

$$CH_2(C_6H_5)_2 \longrightarrow C_{13}H_{10} + H_2 \tag{9}$$

The rate constants for these reactions are not known. However, k_9 has been estimated by Colket and Seery [24] in their modeling of the toluene decomposition. Their estimated value is given in Table I and used in our modeling. The rate constant for reaction (8), which is more important than reaction (9), was obtained by adjusting k_8 to match the experimental and predicted concentrations of H_2 given in Figures 1 and 2 of Ref. 3 over the temperature range 910–1070 K assuming the 0.1% toluene impurity in the reaction mixture. The result gave rise to the expression of $k_8 = 8.35 \times 10^{11} \exp(-11830/T)\ cm^3\ mol^{-1}\ s^{-1}$ and are graphically presented in Figure 3. By assuming the same amount of $C_6H_5CH_3$ impurity present in the mixture, we were able to reasonably predict the yields of H_2 and CH_4 as shown in Figure 4. Similarly, the H_2 yields measured at two temperatures, 923 K and 973 K, as functions of $[C_6H_6]$ could be accounted for by the model, assuming the 0.1% $C_6H_5CH_3$ impurity (see Fig. 5). The slopes of these plots, 1.56 and 1.61 at 923 K and 973 K,

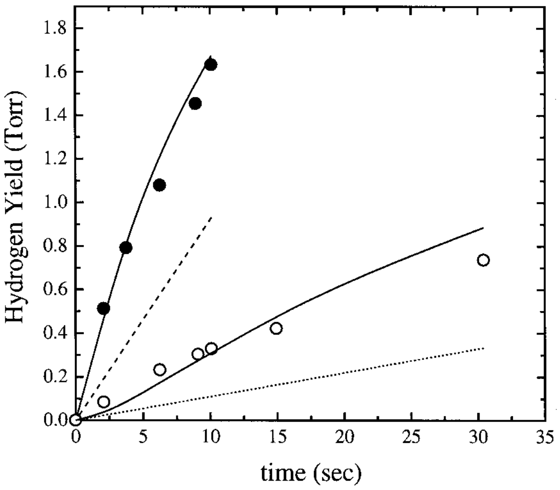

Figure 2 Yields of H_2 with time at 967 K (●) and 910 K (○) for a mixture of 31 Torr benzene and 296 Torr nitrogen. Solid curves, modeling yields of hydrogen with 0.1% toluene impurity in the reaction mixture; dashed (967 K) and dotted (910 K) lines are without toluene impurity.

respectively, confirm the 3/2-order global kinetics observed experimentally. It should be noted that the appearance of CH_4 cannot be accounted for by the ring-opening/fragmentation reactions of C_6H_6 which are of negligible importance at temperature near 1000 K. Interestingly, the 0.1% of toluene impurity is what is required for the enhanced yield of H_2 and the yield of CH_4 measured in the experiment.

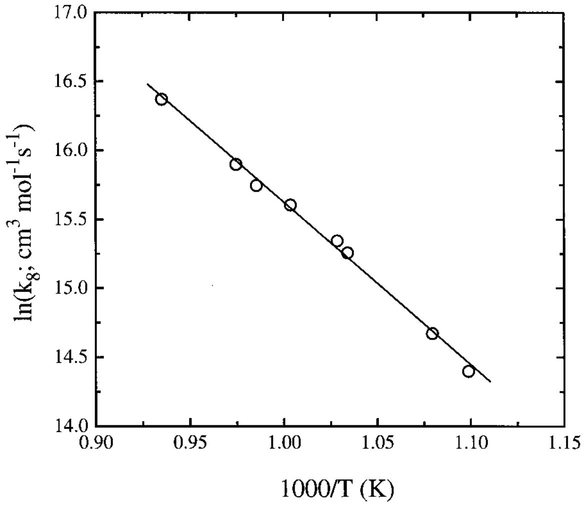

Figure 3 Arrhenius plot of the rate constant for the $C_6H_5CH_2 + C_6H_6 = CH_2(C_6H_5)_2 + H$ reaction (k_8). The rates were obtained by adjusting k_8 values to match the experimental and predicted concentrations of H_2 in Figures 1 and 2 of Ref. 3.

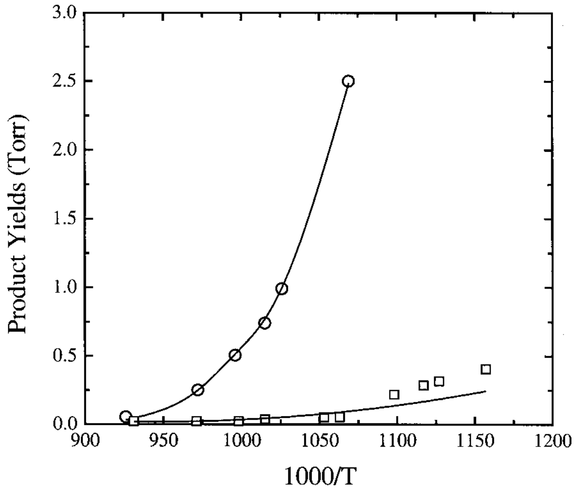

Figure 4 The yields of H_2 (○) and CH_4 (□) as functions of temperature. Solid curves are kinetically modeled results. Reaction conditions: residence time = 60 sec and 31 Torr benzene and 296 Torr nitrogen with 0.1% toluene impurity. The experimental data were taken from Figure 1 of Ref. 3.

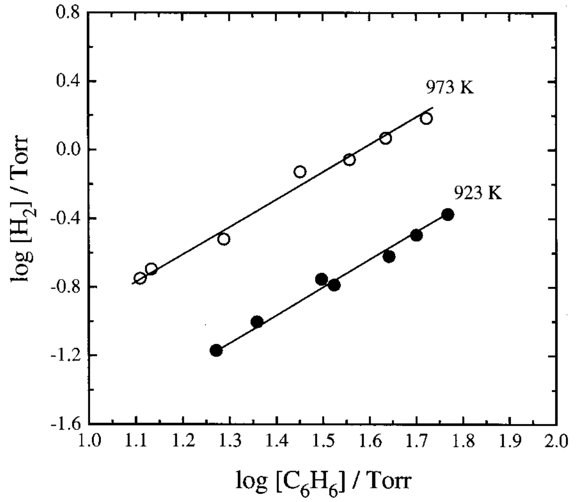

Figure 5 Plot of log [H_2] against log [C_6H_6] measured at 240-sec residence time. Solid lines are modeling results. Total pressure of benzene and nitrogen with 0.1% toluene impurity is 300 Torr.

We have also examined a potential effect of the unimolecular decomposition of C_6H_5:

$$C_6H_5 \longrightarrow o\text{-}C_6H_4 + H$$

which has been predicted theoretically to be the lowest-energy decomposition path (with no reverse barrier), instead of the commonly assumed ring-opening reaction producing an open-chain l-C_6H_5; the activa-

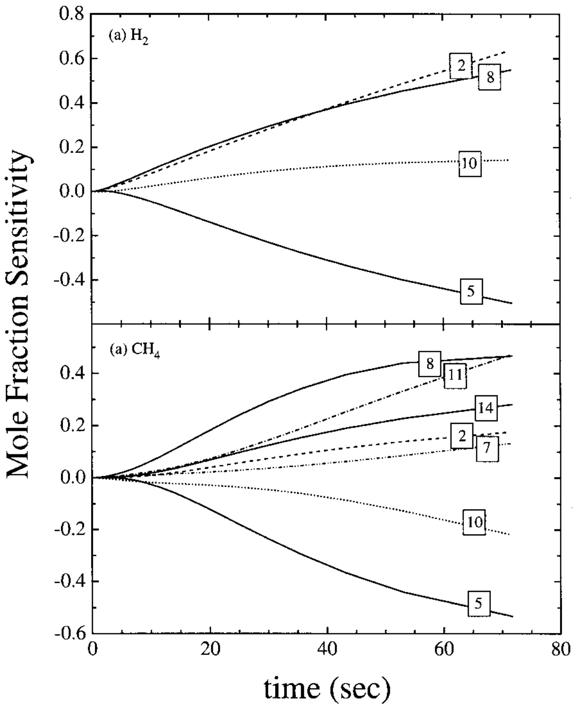

Figure 6 Plots of sensitivity coefficients for H_2 (a) and CH_4 (b) were obtained at $T = 1016$ K, 30.673 Torr benzene, 0.327 Torr toluene and 296 Torr nitrogen.

tion energy of the previous process was calculated to be 78 kcal/mol [25] near 1000 K. However, this secondary reaction was found to be unimportant in the present system.

SENSITIVITY ANALYSIS

We have performed sensitivity analyses for the production of H_2 and CH_4; the results of the analyses at 1016 K are presented in Figure 6. Sensitivity coefficients less than 0.1 are not shown in the figure. For H_2 formation shown in Figure 6(a), H-atom production steps (2) and (8) dominate as expected. The removal of H by H + $C_6H_5CH_2$ (5), negatively affects the yields of H_2.

For CH_4, as revealed by Figure 6(b), reactions (8) and (11) have strong positive effects, whereas reactions (5) and (10) negatively affect the yield of CH_4 as can be expected.

CONCLUSION

The experimentally observed 3/2 kinetics for the dehydrogenation of C_6H_6 near 1000 K by Brooks et al. [3] could be quantitatively accounted for with the four key elementary reactions. However, the presence of the CH_4 product and the enhanced yields of H_2 above the predicted values could only be explained by invoking the reaction of the 0.1% toluene impurity in the reaction mixture reported by the original authors.

This observation suggests that future studies of benzene reaction kinetics should use ultrapure C_6H_6 samples so as to avoid misleading results.

The authors are grateful for the support of this work from the Basic Energy Sciences, Department of Energy, under contract no. DE-FG02-97-ER14784.

BIBLIOGRAPHY

1. Glassman, I. Combustion, 2nd ed.; Academic Press: New York, 1986.
2. Brockhorn, H. Soot Formation in Combustion; Springer-Verlag: New York, 1993.
3. Brooks, C. T.; Peacock, S. J.; Reuben, B. G. J Chem Soc, Faraday Trans I 1979, 75(3), 652.
4. Slysh, R. S.; Kinney, C. R. J Phys Chem 1961, 65, 1044.
5. Hou, K. C.; Palmer, H. N. J Phys Chem 1965, 69, 863.
6. Laskin, A.; Lifshitz, A. 26th Symp. (Int.) on Combustion, The Combustion Institute, 1996, 669.
7. Asaba, T.; Fujii, N. 3rd Symp. (Int.) on Combustion, The Combustion Institute, 1971, 155.
8. Rao, V. S.; Skinner, G. B. J Phys Chem 1984, 88, 5990.
9. Kielfer, J. H.; Mizerka, L. J.; Patel, M. R.; Wei, H.-C. J Phys Chem 1985, 89, 2013.
10. Rao, V. S.; Skinner, G. B. J Phys Chem 1984, 88, 5990.
11. Hsu, D. S. Y.; Lin, C. Y.; Lin, M. C. 20th Symp. (Int.) on Combustion, The Combustion Institute, 1984, 623.
12. Mebel, A. M.; Lin, M. C.; Yu, T.; Morokuma, K. J Phys Chem A 1997, 101, 3189.
13. Park, J.; Dyakov, I. V.; Lin, M. C. J Phys Chem A 1997, 101, 8839.
14. Fahr, A.; Stein, S. E. 22nd Symp. (Int.) on Combustion, The Combustion Institute, 1989, 1023.
15. Manion, J. A.; Tsang, W. Eastern States Section: The Combustion Institute Fall Technical Meeting on Chemical and Physical Processes in Combustion, Dec. 1996.
16. Park, J.; Lin, M. C. J Phys Chem A 1997, 101, 14.
17. Horn, C.; Frank, P.; Tranter, R. S.; Schangg, J.; Grotheer, H.-H.; Just, Th. 26th Symp. (Int.) on Combustion, The Combustion Institute, 1996, 575.
18. Heckmann, E.; Hippler, H.; Troe, J. 26th Symp. (Int.) on Combustion, The Combustion Institute, 1996, 543.
19. Park, J.; Chakraborty, D.; Bhusari, D.; Lin, M. D. J Phys Chem in press.

20. Tokmakov, I. V.; Park, J.; Gheyas, S. I.; Lin, M. D. J Phys Chem in press.
21. Kee, R. J.; Rupley, F. M.; Miller, J. A. CHEMKIN-II: A FORTRAN Chemical Kinetics Package, for the Analysis of Gas-Phase Chemical Kinetics, Sandia National Laboratory Report No. SAND 89-8009, 1988.
22. Lutz, A. E.; Kee, R. J.; Miller, J. A. SENKIN: A FORTRAN Program for Predicting Homogeneous Gas-Phase Chemical Kinetics with Sensitivity Analysis, Sandia National Laboratory Report No. SAND 87-8009, 1989.
23. Melius, C. F. http://herzherg.sandia.gov/∼melius.
24. Colket, M. B.; Seery, D. J. 25th Symp. (Int.) on Combustion, The Combustion Institute, 1994, 883.
25. Madden, L. K.; Moskaleva, L. V.; Kristyan, S.; Lin, M. C. J Phys Chem A 1997, 101, 6790.
26. Baulch, D. L.; Cobos, C. J.; Cox, R. A.; Esser, C.; Frank, P.; Just, Th.; Kerr, J. A.; Pilling, M. J.; Troe, J.; Walker, R. W.; Warnatz, J. J Phys Chem Ref Data 1992, 21, 411.
27. Tsang, W.; Kiefer, J. H. In The Chemical Dynamics and Kinetics of Small Radicals, Pert, I; Liu, K.; Wager, A. Eds.; Chapter 3, 1995; pp 58–119.
28. Dunlop, A. N.; Kominar, R. J.; Price, S. J. W. Can J Chem 1970, 48, 1269.
29. Muller-Markgraf, W.; Troe, J. J Phys Chem 1988, 92, 4899.
30. Braud, U.; Hippler, H.; Lindermann, L.; Troe, J. J Phys Chem 1990, 94, 6305.
31. Cohen, N.; Westberg, K. R. J Phys Chem Ref Data 1983, 12, 531.